Hindawi Publishing Corporation
International Journal of Photoenergy
Volume 2011, Article ID 869589, 9 pages
doi:10.1155/2011/869589

Research Article

Conversion of Dagang Vacuum Residue into Oxygen-Containing Organic Compounds by Photo-Oxidation with H_2O_2 over TiO_2

Heng-Shen Xie,[1,2] Zhi-Min Zong,[1] Qing Wei,[1] Tong Liu,[1] Jian-Jun Zhao,[1] Pei-Zhi Zhao,[1] Shi-Hua Zhang,[1] and Xian-Yong Wei[1,3]

[1] *Key Laboratory of Coal Processing and Efficient Utilization (Ministry of Education), China University of Mining and Technology, Xuzhou, Jiangsu 221008, China*
[2] *Division of Science & Technology, Xuzhou Institute of Architectural Technology, Xuzhou, Jiangsu 221116, China*
[3] *Hubei Coal Conversion and New Carbon Materials Key Laboratory, Wuhan University of Science and Technology, Wuhan, Hubei 430081, China*

Correspondence should be addressed to Xian-Yong Wei, wei_xianyong@163.com

Received 26 October 2010; Revised 19 January 2011; Accepted 21 April 2011

Academic Editor: J. Anthony Byrne

The photocatalytic depolymerization of Dagang vacuum residue (DVR) was carried out with H_2O_2 over TiO_2 in a photochemical reactor. Most of the organic matter in DVR was converted into oxygen-containing organic compounds. The yields of carboxylic acids, oxalates, epoxy compounds, and hydroxyl compounds from DVR oxidation are 40.6%, 36.4%, 17.86%, and 13.5%, respectively. In addition, the oxidation causes significant decrease in viscosity and chromaticity of DVR. The related reaction mechanisms are discussed according to the experimental results.

1. Introduction

Heavy oil becomes more and more important with rapid reduction of light oil and drastic increase of liquid fuels [1–5]. As typical heavy oil in China, Dagang vacuum residue (DVR) has high viscosity and chromaticity [6].

Photo-catalytic oxidation (PCO) has been widely applied to many aspects such as solar energy transformation, environmental protection and the syntheses of coating, cosmetic and printing ink, food-packaging materials, gas sensors and functional ceramics [7–15]. Almost all the organic matter (OM) in aqueous solution can be converted into carbon dioxide and water by PCO; hydroxyl oxidation and electron-hole pair oxidation are principal processes in the course of oxidation [16–18]. However, selective PCO of heavy oil in organic solvent has not been reported to our knowledge. In the present study, we found that OM in DVR can be converted into oxygen-containing organic compounds (OCOCs), which can be used as industrial raw materials for the synthesis of dyes and medicines. Particularly, dialkyl oxalates in the OCOCs are reactive intermediates for preparing chemical cold light source [19–22].

2. Experimental Section

2.1. Samples and Reagents. DVR, the residue of crude oil vacuum distillated later and collected from Dagang Oil Field, Tianjin Municipality, China, was preserved in sealed condition. Table 1 shows the elementary properties and ultimate analysis of DVR. Cyclohexane, acetone, and hydrogen peroxide (30% wt) are commercial purchased analytical reagents, and all organic solvents used in the experiment were distilled prior to use. Titanium dioxide as photocatalyst was prepared by Sol-Gel method and characterized by ultraviolet visible (UV-VIS), X-ray diffraction (XRD), and transmission electron microscopy (TEM) (as shown in Figures SI-1, 2, 3, and 4 and Table SI-1, see Supplementary Materials available at doi:10.1155/2011/869589), implying the homemade powders are anatase nanometer particles, and its particle radius is no more than 20 nm, and its properties are similar to the commercial reagent P-25 [23].

2.2. Instruments and Equipment. The SGY-1 multifunctions photochemistry reactor with the function of rotating and with 500 W low-pressure mercury lamp as light source, which can emit around 85% ultraviolet light with wavelength

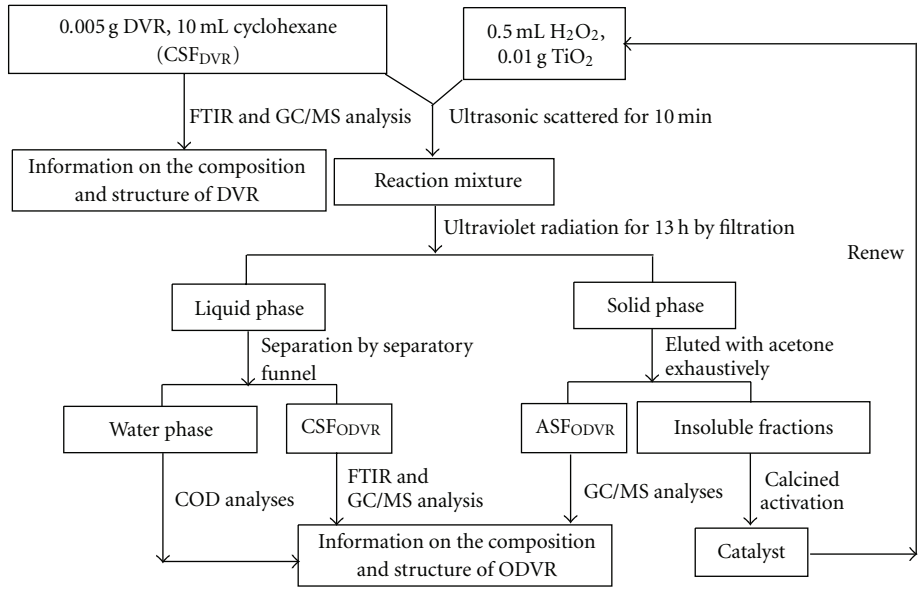

Figure 1: Procedure for DVR oxidation, subsequent treatment, and products analysis.

of 365 nm (its energy distribution as shown in Table SI-8), was made in Nanjing Sidongke Electric Equipment Co. of China. The reactor was used to study the quantum yield of photochemistry reaction, especially the synthesis of new materials or the degradation of organic contaminations (as Figure SI-7). The instruments for analyses of products are a Nicolet Magna IR-560 Fourier transform infrared (FTIR) and a Hewlett-Packard 6890/5973 gas chromatography/mass spectrometer (GC/MS) equipped with a capillary column coated with HP-5 (cross-link 5% PH ME siloxane, 30 m × 0.25 mm i.d., 0.25 μm film thickness) and a quadrupole analyzer and operated in electron impact (70 eV) mode.

2.3. Photochemical Treatment and Analyses Method. As shown in Figure 1, 0.005 g of DVR was dissolved in 10 mL cyclohexane and mixed with TiO_2 (amount of 0.01 g) and H_2O_2 (ca. 0.5 mL). The mixtures were dispersed under ultrasonic for 10 min and illuminated with 500 watt low-pressure ultraviolet mercury lamp for 13 hours in electromagnetic stirring. Then the reaction mixture was filtered and separated and eluted with cyclohexane and acetone, respectively. The cyclohexane-soluble fraction (CSF_{ODVR}) and the acetone-soluble fraction (ASF_{ODVR}) were analyzed with GC-MS or FTIR. The residue was calcined to obtain the service life of catalyst. The chemical oxygen demand (COD) of the aqueous soluble was determined using titration with potassium dichromate. In addition to the model compounds such as liquid paraffin, decahydronaphthene and tetrahydronaphthalene were oxidized by UV light to analyze the depolymerization mechanism of DVR photo-catalytic oxidation under the same condition. The reaction results of model compounds were shown in Tables SI 3, 4 and 5. And the reaction results of DVR were also discussed with FTIR analyses.

3. Results and Discussion

3.1. Analysis of Cyclohexane Photo-Oxidation. Different solvents have different polarity and stability, especially when they are illuminated by UV light. DVR mainly consists of low-polarity alkyl saturated hydrocarbon. Hence, cyclohexane with lower polarity and stability to UV light is selected as solvent in PCO according to similar dissolve mutually theory. Of course, the products from the PCO of cyclohexane may have effect on the analysis result of ODVR. So in order to eliminate the interference, the cyclohexane was oxidized alone by photo-catalytic oxidation and with GC/MS analyses. The result is exhibited in Figure 2, the oxidation products are listed in Table SI-2. As shown Figure 2, in total six products were identified, including cyclohexanol, cyclohexanone, cyclohexyl formate, cyclohexylcyclohexane, (cyclohexyloxy)cyclohexane, and cyclohexyl hexanoate. Among the oxidation products the relative contents of compound 6 ((cyclohexyloxy)cyclohexane) and compound 2 (cyclohexanol) are higher and account for 14.30% and 5.76%, respectively. However, no 1-cyclohexylcyclohex-1-ene, cyclohexene, and cyclohexy-lidenecyclohexane were detected, implying active hydrogens in cyclohexane ring can be substituted partly by hydroxyl radicals to form cyclohexane derivatives, but the derivatives are difficult to eliminate and to form the products of cyclohexane ring opening or unsaturated compounds. The mechanism of product formation is represented in Scheme 1. Where the solvent is not oxidized under the mild conditions, present selection of solvent is more appropriate.

3.2. Effect of TiO_2 on DVR Oxidation by FTIR Analysis. As shown in Figure 3, no absorbance at 3480 cm^{-1} was observed in E_I (the system of DVR cyclohexane solution) and E_{II} (the system of DVR cyclohexane solution oxidized with

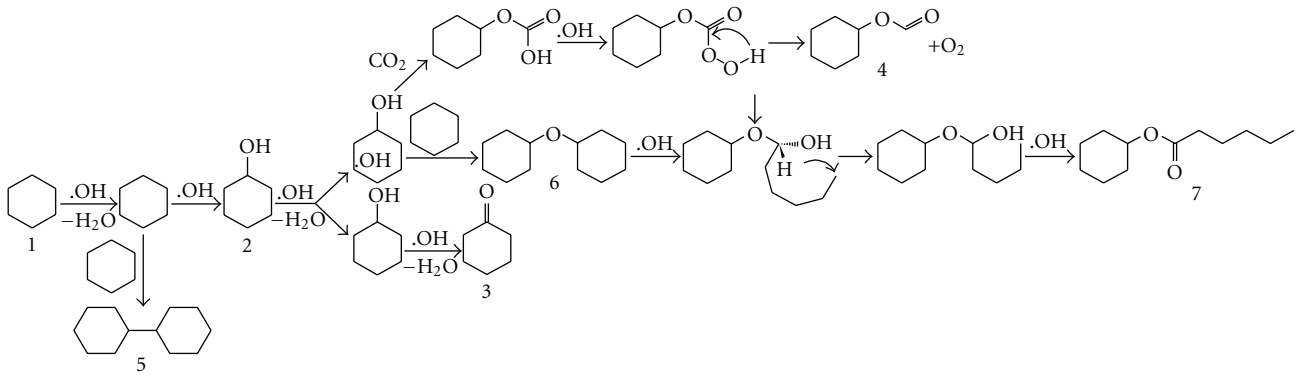

Scheme 1: Mechanism for the degradation of cyclohexane in PCO.

Table 1: Property and ultimate analyses of DVR.

DVR property				Elemental composition (wt%, daf)				
RC (%)	D (g cm^{-3})	V (mPas)	MM	C	H	N	S	O*
17.02	0.9796	2074	1008	85.91	11.43	0.61	0.24	1.81

RC: residual carbon; *D:* density; *V:* viscosity; MM: molecular mass; *by difference.

Table 2: Alkenes detected in the products from CSF_{DVR} and ASF_{ODVR}.

Peak	Alkene	Detected in	
		CSF_{DVR}	ASF_{ODVR}
54	(E)-icos-7-ene	2.2	
68	Octadec-1-ene		1.0
71	Docos-1-ene		0.2
76	(E)-octadec-7-ene	1.2	
86	(E)-henicos-10-ene		0.7
93	Nonadec-1-ene	3.8	0.5
104	Squalene	8.0	

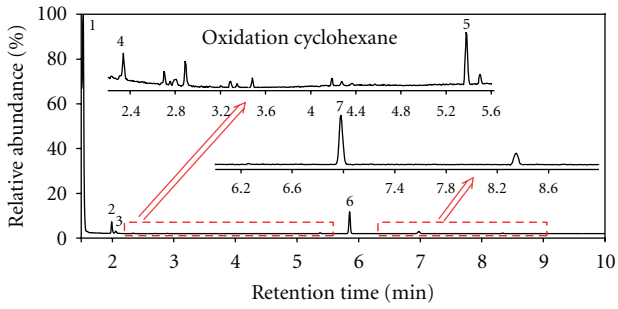

Figure 2: Total ion chromatograms of oxidation cyclohexane.

H_2O_2), but a broad absorption band in E_{III} (the system of DVR cyclohexane soluble oxidized with H_2O_2 over TiO_2), which suggests that the concentration of hydroxyls produced by the synergistic effect of TiO_2 and H_2O_2 is higher. The absorbance at 1730 cm^{-1} is found in E_{II}, and E_{III} and the peak is stronger in E_{III} than in E_{II}, indicating C=O as a functional group in oxidation products, and the oxidation effect is obvious in E_{III}. This shows that oxidation of DVR requires both TiO_2 and peroxide for successful oxidation. Peaks at 3480 cm^{-1}, 2930 cm^{-1}, 2860 cm^{-1}, 1370 cm^{-1}, and 1460 cm^{-1} are very strong, only with different strength, suggesting that $-CH_3$ and $=CH_2$ exist in CSF_{DVR}, CSF_{ODVR}, and ASF_{ODVR} and with different contents. It proved the formation of –OH, and the existence of hydroxyl oxidation was included in E_{II} and in E_{III}. As far as two systems, the absorbances at 1730 cm^{-1} were attributed to the carbonyl compounds, but the intensity in E_{III} is stronger than in E_{II}, indicating higher concentration of carbonyl groups and the oxidation effect of DVR more obviously. The absorbance at 2380, 2330 cm^{-1} in cyclohexane and E_I, but not in E_{II}, was found, illustrating that C=C has been converted into saturation hydrocarbon or other OOCs. Hence, most of OMs in DVR have been converted into high-polarity compounds. Especialy, the conversion in E_{III} is the most effective because of the synergistic effect. The conclusion also depends on GC/MS analyses and verification.

3.3. GC/MS Analysis of DVR and Oxidation Products. The compounds detected in CSF_{DVR}, CSF_{ODVR}, and ASF_{ODVR} were listed in Tables 2–11 and Tables SI-3 and 4. The total ion chromatograms (TICs) were presented in Figures SI-5 and 6. 27 species compounds in CSF_{DVR}, 21 species compounds in CSF_{ODVR}, and 73 species compounds in ASF_{ODVR} were detected. Their parent compounds can be classified normal alkanes (NAs), branched-chain alkanes (BAs), esters, carbonyl acids, alkenes, arenes, ketones, alcohols, phenols and epoxy compounds (ECs). Compounds 99, 51, and 5 are the most abundant in CSF_{DVR}, CSF_{ODVR}, and ASF_{ODVR}, respectively; they are dotriacontane, allyl tetradecyl oxalate, and 4-oxopentanoic acid, in sequence accounting for 10.02%, 13.47%, and 25.14%. As shown in Figures SI-5 and 6 and Tables 2–10, OMs in CSF_{DVR} were converted into polar OOCs in CSF_{ODVR} or in ASF_{ODVR} via PCO.

Table 3: Monobasicacidesters detected in the products from ASF_{ODVR}.

Peak	Monobasic acid ester	Detected in
14	Dihydro-4-hydroxyfuran-2(3H)-one	2.1
17	Dihydro-5-(hydroxymethyl)furan-2(3H)-one	1.2
19	2-hydroxycyclohexyl acetate	0.7
24	4-hydroxycyclohexyl acetate	0.6
31	(3Z,11Z)-octadeca-3,11-dienyl acetate	0.3
35	4-methylpentyl pentanoate	5.2
36	Octan-4-yl hexanoate	2.0
38	5,6-dihydro-4-(2-methylprop-1-enyl)pyran-2-one	0.2
48	Sec-butyl phenyl carbonate	0.1
72	Heptadecyl 2,2,2-trifluoroacetate	0.4
79	Etradec-13-enyl acetate	0.2

Table 4: Dialkyl alkanedioates in the products from CSF_{ODVR} and ASF_{ODVR}.

Peak	Dialkyl alkanedioate	Detected in	
		CSF_{ODVR}	ASF_{ODVR}
22	Trans-cyclohexane-1,4-diyl-diacetate		0.4
49	Dodecyl isobutyl oxalate	7.2	
51	Allyl tetradecyl oxalate	13.5	
58	Cyclobutyl octadecyl oxalate	4.7	
63	Dicyclohexyl malonate		1.0
73	Cyclobutyl pentadecyl oxalate	3.7	
77	Isobutyl pentadecyl oxalate	5.7	
84	Hexadecyl isobutyl oxalate	5.8	

As listed in Table SI-3, in total 18 NAs (C_{14}–C_{36}) were affirmed in CSF_{DVR}, CSF_{ODVR}, and ASF_{ODVR}. As Figures SI-5 and 6 show the TICs spectra of CSF_{DVR}, CSF_{ODVR}, and ASF_{ODVR}, 16 NAs were identified in CSF_{DVR}, accounting for 65.67%, indicating DVR mainly composed of NAs. It is considered that it is difficult for NAs to oxidize in mild condition, but the RC of NAs in CSF_{ODVR} and ASF_{ODVR} was reduced dramatically. Only 8 NAs in CSF_{ODVR} and 5 NAs in ASF_{ODVR} were detected, accounting for 41.55% and 2.1%, respectively. So we assumed that the NAs have been converted into other OOCs in the experiment. Through the photo-catalytic oxidation degradation of model compounds, liquid paraffin indicates that NAs can be converted into OOCs including alcohols and α-unsaturated chain hydrocarbons.

As shown in Tables SI-4 and 5 BAs, accounting for 12.22%, were detected in CSF_{DVR}. After PCO about a quarter BAs were reduced in CSF_{ODVR} in relative to in CSF_{DVR}, less than 2% BAs was detected in ASF_{ODVR}. These data indicate that BAs participated in the reaction of photo-oxidation. BAs with large amounts of active hydrogen were subject to

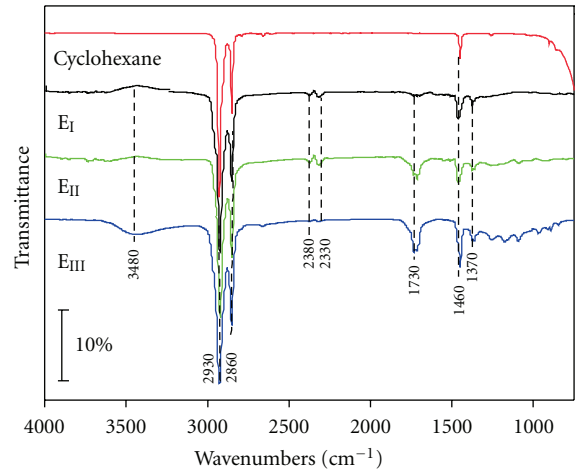

Figure 3: FTIR spectra of cyclohexane and DVR oxidized before and later.

substituting by hydroxyl free radicals formation hydroxyl compounds (HCs) or eliminating dehydration by electron-hole pairs in the process of PCO. It is obvious that part BAs may be formed in the course of PCO degradation, so BAs can be detected in CSF_{ODVR} and ASF_{ODVR} though they are easy to be degraded.

As shown in Table 2, alkenes is a vital component in CSF_{DVR}, only 4 alkenes, accounting for 15.19%, were detected. The RC of alkenes in ASF_{ODVR} was 2.4% though 4 alkenes were determined, while no alkenes were observed in CSF_{ODVR}. The analysis result of GC/MS indicate that these alkenes with high-ploarity in contrast to cyclohexane are unstable under UV light irradiation, they participate in photo-oxidation degradation reaction by two processes of the oxidation of hydroxyl radicals and Michael' addition reaction.

As shown in Tables 3–5, in total 23 esters were determined in CSF_{ODVR} and ASF_{ODVR} and no OEs was detected in CSF_{DVR}, suggesting that OEs are the main oxidation products. In them, 6 OEs (including dodecyl isobutyl oxalate, allyl tetradecyl oxalate, cyclobutyl octadecyl oxalate, cyclobutyl pentadecyl oxalate, isobutyl pentadecyl oxalate, and hexadecyl isobutyl oxalate) were identified in CSF_{ODVR}, and the total RC is 40.55%, indicating the formation of oxalate functional groups in PCO (as shown in Figure 4, the mass spectra of the oxalic esters). In addition, 16.34% of 17 OEs were also detected in ASF_{ODVR}, indicating that heavy oil has been converted successfully by PCO. Because of the existence of carbonyl acids (CAs) and alcohols as shown in Tables 8 and 9, OEs are possibly generated through the esterification of acids and alcohols. It is unlikely generation from the openingring of ACs' hydroxylation derivatives because the photo-catalytic oxidation degradation of model compounds did not discover the open-loop product (as shown in Tables SI-5 and 6 PCOs of decahydronaphthene and tetrahydronaphthalene). And the formation of OEs proved that DVR can be converted into OOCs successfully through several methods. OEs, as terminal OOCs, are easy to isolate from nonpolar materials, so they are important

Table 5: Dialkyl phthalates detected in the products from ASF_{ODVR}.

Peak	Dialkyl phthalate	Detected in	Peak	Dialkyl phthalate	Detected in
52	Diethyl phthalate	0.5	**74**	Butyl octyl phthalate	0.4
57	Diisobutyl phthalate	0.9	**91**	Bis(6-methylheptyl)phthalate	0.1

Table 6: Acids detected in the products from ASF_{ODVR}.

Peak	Acid	Detected in	Peak	Acid	Detected in
2	Hexanoic acid	0.4	**33**	Oxepane-2,7-dione	3.7
5	4-oxopentanoic acid	25.1	**40**	Dodecanoic acid	0.2
12	5-oxohexanoic acid	1.6	**45**	Tridecanoic acid	0.3
13	3-(ethoxycarbonyl)propanoic acid	0.8	**47**	Tetradecanoic acid	0.4
15	1,3-dioxol-2-one	0.4	**56**	Pentadecanoic acid	0.3
23	Succinic acid	0.1	**64**	n-hexadecanoic acid	0.3
27	Glutaric acid	3.0	**65**	Palmitic acid	0.3

Table 7: Alcohols detected in the products from CSF_{DVR}, CSF_{ODVR} and ASF_{ODVR}.

Peak	Alcohol	Detected in		
		CSF_{DVR}	CSF_{ODVR}	ASF_{ODVR}
6	(1R,2R)-cyclohexane-1,2-diol			2.9
11	2,2-dimethyloctan-3-ol			5.9
16	4-methylheptan-3-ol			1.0
29	2,5-dimethylhex-4-en-3-ol			0.2
30	Tridecan-7-ol			0.4
39	2-octadecylpropane-1,3-diol		0.7	
60	Hexadecane-1,2-diol			0.2
62	2-methyl-5,5-diphenylpenta-3,4-dien-2-ol			0.3
90	2-(octadecyloxy)ethanol	2.0	1.9	

Table 8: Phenols detected in the products from ASF_{ODVR}.

Peak	Phenol	Detected in
3	Phenol	0.1
88	2,4-bis (2-phenylpropan-2-yl)phenol	1.4

industrial raw materials. Among them, oxalates always are considered as a main intermediate to make the cold light illuminator or other military supplies. Hence, the conversion of compounds in PCO provides an effective approach to make the DVR utilization effective.

As listed in Table 6, CAs are one of the OOCs and merely detected in ASF_{ODVR}, suggesting that CAs as final products are strongly polarity matters. As Figure 5 has shown that the RC of CAs is 36.4%, and compound 5 (shown in Figure SI-6 and in Figure 5) is the most abundant account for 25.58% in ASF_{ODVR}. OKs and ACs were also detected only in ASF_{ODVR}, as shown in Tables 9 and 10, and the RC of them is 8.79% and 1.13%, respectively, indicating that carbonyl compounds have been formed in the reaction, and the primary products can react continuously with each other through the addition reaction cyclopolymerization. From the upper analysis result, we suppose that the solvent participated in the reaction but without the formation of ring opening components. The formation of compounds containing cyclohexane provided a proof that the active hydrogens were attacked by hydroxyls and obtained the production of cyclohexyl free radicals.

As illustrated in Tables 7 and 8, in total 10 HCs (including alcohols and phenols) were detected, among them, one HC in CSF_{DVR}, 2 HCs in CSF_{ODVR} and 7 HCs in ASF_{ODVR}. In ASF_{ODVR} 2,2-dimethyloctan-3-ol (compound 11 in Figure SI-6) is the most abundant, accounting for ~5.94% of OMs, while ~1.86% of OMs in CSF_{ODVR}. The formation of (1R,2R)-cyclohexane-1,2-diol suggests that OMs in DVR can be oxidized by hydroxyl substitution besides cyclohexane. These facts indicate that hydroxyl oxidation is a main step in photo-oxidation process. It must be considered as the mechanism causing the ring-opening reaction of cyclohexane, but the products of ring opening were almost not detected in the products of pure cyclohexane oxidation, so it is sure that active hydrogen in DVR has been substituted by hydroxyl free radicals and led to the formation of these HCs. The RC of HCs in CSF_{ODVR} is less than that in ASF_{ODVR}, indicating the HCs with high polar. In addition, one HC exists in CSF_{DVR}, and it is unsteady and easy to depolymerization.

As listed in Table 11, in total 11 ECs were detected 2-((dodecyloxy)methyl)oxirane appeared both in CSF_{DVR} and CSF_{ODVR} simultaneously, whereas 10 ECs were detected in

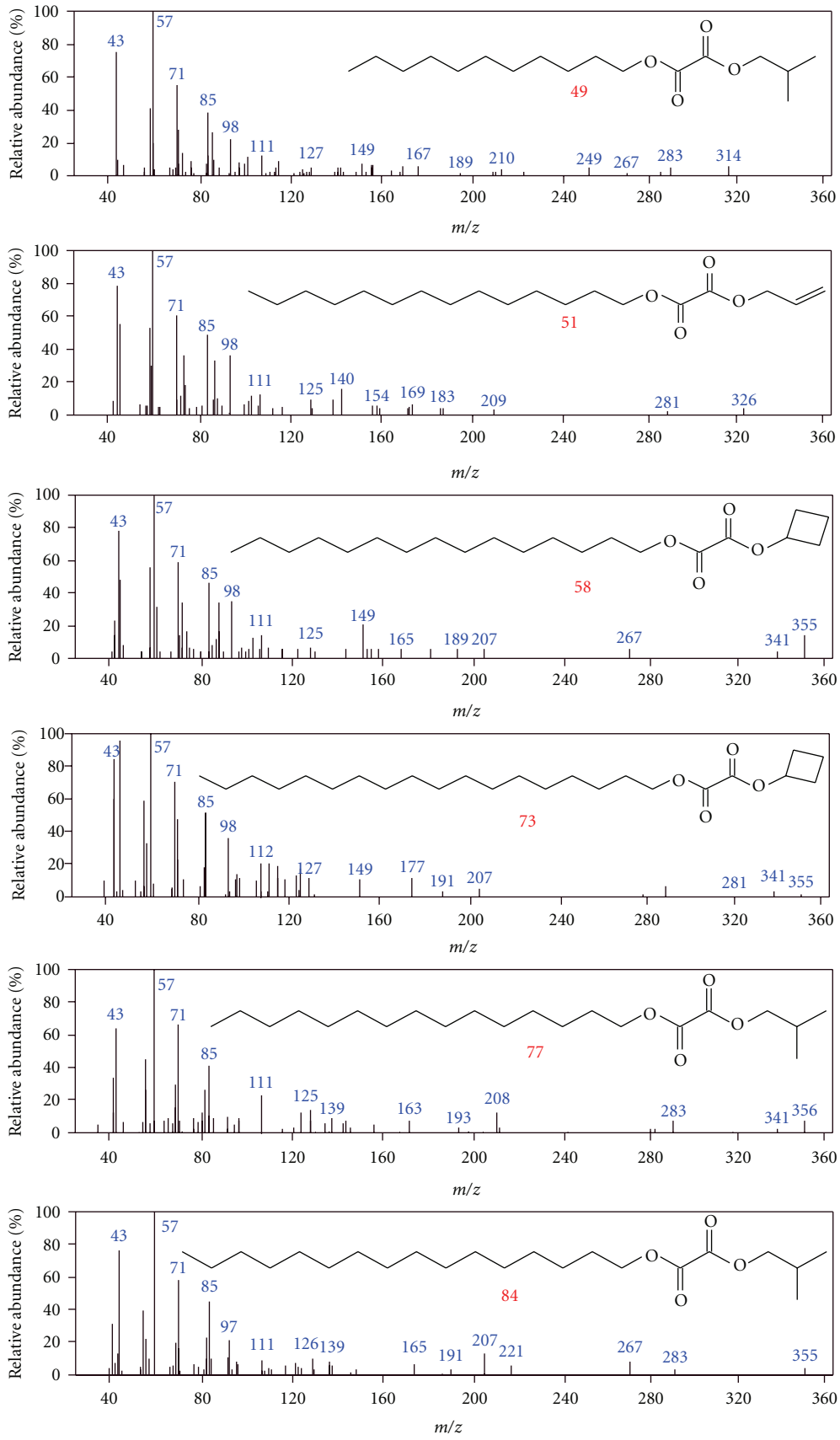

Figure 4: Mass spectra of the dialkyl oxalates detected in CSF_{ODVR}.

Table 9: Ketones detected in the products from ASF_{ODVR}.

Peak	Ketone	Detected in	Peak	Ketone	Detected in
1	Cyclohex-2-enone	0.6	**32**	3-hydroxycyclohexanone	7.2
8	Cyclohexane-1,4-dione	0.3	**38**	5,6-dihydro-4-(2-methylprop-1-enyl)pyran-2-one	0.2
10	4-hydroxycyclohexanone	0.3	**75**	Anthracene-9,10-dione	0.6

Table 10: ACs detected in the products from ASF_{ODVR}.

Peak	AC	Detected in	Peak	AC	Detected in
9	(4as,8as)-decahydronaphthalene	0.7	**55**	Phenanthrene	0.1
53	Anthracene	0.2	**81**	9,10-dichloroanthracene	0.1

Table 11: ECs detected in the products from CSF_{DVR}, CSF_{ODVR} and ASF_{ODVR}.

Peak	Epoxy compound	Detected in		
		CSF_{DVR}	CSF_{ODVR}	ASF_{ODVR}
4	dihydrofuran-2,5-dione			6.7
7	2-propylfuran			0.4
18	3,4-dimethylfuran-2,5-dione			0.3
21	4,5-dimethyl-2-pentadecyl-1,3-dioxolane			0.4
25	tetrahydro-3-methyl-5-oxofuran-2-carboxylic			5.8
26	isobenzofuran-1,3-dione			1.5
28	tetrahydro-5-oxofuran-2-carboxylic acid			0.5
34	5-heptyl-dihydrofuran-2(3H)-one			1.4
46	dihydro-5-(hydroxymethyl)furan-2(3H)-one			0.5
87	3-(tetrahydro-5-oxofuran-2-yl)propanoic			0.3
97	2-((dodecyloxy)methyl)oxirane	4.9	6.3	

ASF_{ODVR} and most of them are rich with pentaheterocycles (such as furan, lactone, and acid anhydrides). The reason is that the electron pair in hydroxyl oxygen atoms attacked the active hydrogen in the same link and formed a ring and then formed the stable structure in organic molecular on account of losing the proton. This is the electrophilic substitution reaction. Furthermore, the relative content of penta-heterocycles is the highest (account for 17.82%) mainly because of the small ring strain and the stable ring structure [24].

3.4. Mass Spectra Analyses of Oxalate in CSF_{ODVR}. As exhibited in Figure 4, six oxalates in CSF_{ODVR} were identified with large number of RC. These compounds in peaks 49, 51, 58, 73, 77, and 84 (as shown in Figure SI-5) seem to be oxalate containing because of the fragments at m/z 207. The molecular ions M+ at m/z 356 are compounds 73 and 77, and compound 49 is at m/z 314 and compound 51 is at m/z 326, but the molecular ions of the compounds 58 and 84 disappear. If the peak at m/z 207 was considered as column loss or other impurity peaks, the mass spectra shape of oxalates should be similar to that of NAs. However, the oxalates were determined with GC/MS analyses and acquired processes using Chemstation software with NIST05 library data. In addition, the structure of compounds 58 and 73 is cis-, but the structures of compounds 49, 51, 77, and 84 are trans-, indicating the cis-formation of oxalates with cyclobutane as branched-chain more stable than the corresponding trans-forms. However, the trans-formation of oxalates with branched chain alkanes or unsaturated is more stable than the corresponding trans-forms. The possible reason is that the substitutions meet with different steric hindrance. The stereohindrance effect of cyclobutane and the repulsion force between a pair of electrons cause the carbon-carbon bond formation in oxalate rotation.

3.5. Mechanics of Photo-Oxidation Degrading DVR. As shown in Figure 5, five species OMs in CSF_{DVR} were converted into five species of OMs in CSF_{ODVR} and nine species of OMs in ASF_{ODVR}, presenting the diversified products formed. Key steps of the products transformation are as follows. Firstly, the active hydrogen from methyl or methylene in NAs, BAs or branched-chain aromatics could be substituted by the hydroxyls generated on the surface of TiO_2 with H_2O_2 in the process priority, and lead to form HCs. Some HCs eliminate water molecular to form UCs, and UCs in ASF_{ODVR} product easily undergo Michael addition reaction and generate lactone rings or cyclic ethers (such as furan or acid anhydrides). In addition, some HCs or UCs can also be converted into OKs or CAs and other OEs by hydroxyl radicals attack. The facts proved that alkanes, not only BAs or ACs with branched chain, can be oxidized in the processes. Secondly, the biomarkers through bond breaking, ring opening, and small molecules eliminated could be

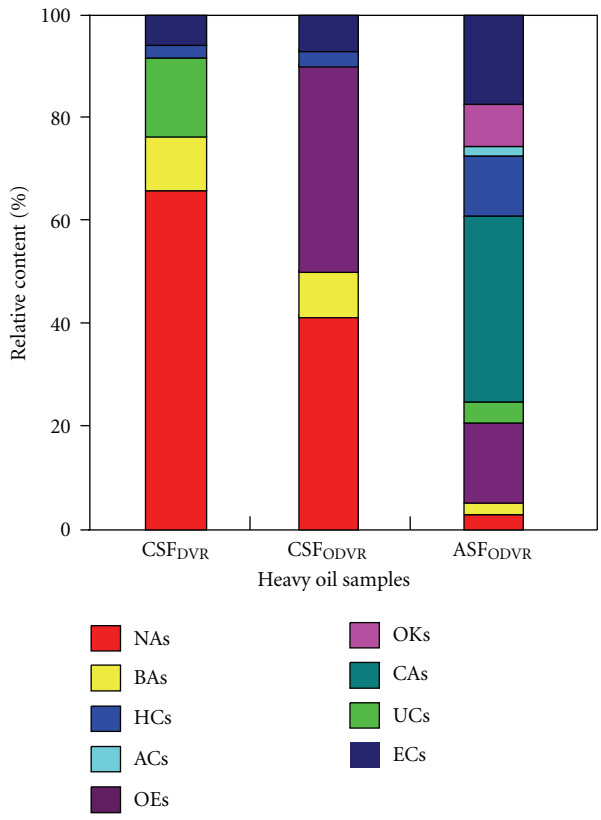

Figure 5: Distributions of group components in solution of CSF$_{DVR}$, CSF$_{ODVR}$and ASF$_{ODVR}$.

oxidized into ACs. Thirdly, deep oxidation or elimination proved that HCs and UCs have been converted into CAs or OEs. Fourthly, esterification of CAs and HCs causes the yield of OEs. Finally, the reaction between UCs and HCs is Michael addition reaction.

4. Conclusions

Most of OMs in DVR was depolymerized and converted into high-polarity OOCs successfully, which are soluble species in cyclohexane or acetone through PCO, and their relative contents reach above 92%. Even NAs can be also oxidized to form HCs in PCO, and their contents decrease from 65.67% to 44.55%.

Main products of OOCs, including CAs, OEs, HCs, and OKs, are all essential industry materials. As for oxalates, it can be used as the intermediate to make chemical cold-light illuminator. So PCO depolymerization of DVR is an effective way, not only to analyze the structure of DVR but also to realize the effective conversion or application of DVR.

The color of system and the viscosity of DVR were reduced gradually with the generating of hydroxyl radicals in the photo-catalytic oxidation reaction. The change of DVR color, viscosity, and polarity is favorable to solve environmental protection question, which is caused by heavy oil in the course of transportation, reserving, and utilizing. The synergistic effect of TiO_2 and H_2O_2 is the most effective to the reaction.

Acknowledgment

This work was supported by the Special Fund for Major State Basic Research Project (Project no. 2004CB217601), National Natural Science Foundation of China (Project no. 50974121), and the Program of the Universities in Jiangsu Province for Development of High-Tech Industries (Project no. JHB05-33).

References

[1] D. G. Lee and N. A. Noureldin, "Effect of water on the low-temperature oxidation of heavy oil," *Energy & Fuels*, vol. 3, no. 6, pp. 713–715, 1989.

[2] M. Xiang-Hai, X. Chun-Ming, L. Li, and G. Jin-Sen, "Studies on the kinetics of heavy oil catalytic pyrolysis," *Industrial and Engineering Chemistry Research*, vol. 42, no. 24, pp. 6012–6019, 2003.

[3] S. R. Stoyanov, S. Gusarov, S. M. Kuznicki, and A. Kovalenko, "Theoretical modeling of zeolite nanoparticle surface acidity for heavy oil upgrading," *Journal of Physical Chemistry C*, vol. 112, no. 17, pp. 6794–6810, 2008.

[4] A. Ambalae, N. Mahinpey, and N. Freitag, "Thermogravimetric studies on pyrolysis and combustion behavior of a heavy oil and its asphaltenes," *Energy and Fuels*, vol. 20, no. 2, pp. 560–565, 2006.

[5] E. Fumoto, A. Matsumura, S. Sato, and T. Takanohashi, "Recovery of lighter fuels by cracking heavy oil with zirconia-alumina-iron oxide catalysts in a steam atmosphere," *Energy and Fuels*, vol. 23, no. 3, pp. 1338–1341, 2009.

[6] Y. Q. Wang, L. X. Zhou, Z. M. Zong et al., "Synergistic catalytic hydrogenation of catalysts co-operation on the draff from supercritical fluid extraction of Dagang vacuum residue," *Applied Chemical Industry*, vol. 35, no. 11, pp. 887–892, 2006.

[7] A. Fujishima and K. Honda, "Electrochemical photolysis of water at a semiconductor electrode," *Nature*, vol. 238, no. 5358, pp. 37–38, 1972.

[8] N. C. Han, S. H. Cho, Y. J. Park, W. L. Dai, and W. Y. Lee, "Sol-gel-immobilized Tris(2,2-bipyridyl)ruthenium(II) electrogenerated chemiluminescence sensor for high-performance liquid chromatography," *Analytica Chimica Acta*, vol. 541, no. 1–2, pp. 47–56, 2005.

[9] M. R. Hoffmann, S. T. Martin, W. Choi, and D. W. Bahnemann, "Environmental applications of semiconductor photocatalysis," *Chemical Reviews*, vol. 95, no. 1, pp. 69–96, 1995.

[10] O. Legrini, E. Oliveros, and A. M. Braun, "Photochemical processes for water treatment," *Chemical Reviews*, vol. 93, no. 2, pp. 671–698, 1993.

[11] Y. Inel and I. A. Balcioglu, "Photocatalytic degradation of organic contaminated in semiconductor suspensions with added H_2O_2," *Journal of Environmental Science and Health, Part A*, vol. 31, no. 1, pp. 123–128, 1996.

[12] R. Asahi, T. Morikawa, T. Ohwaki, K. Aoki, and Y. Taga, "Visible-light photocatalysis in nitrogen-doped titanium oxides," *Science*, vol. 293, no. 5528, pp. 269–271, 2001.

[13] G. Li Puma and P. L. Yue, "A novel fountain photocatalytic reactor: model development and experimental validation,"

Chemical Engineering Science, vol. 56, no. 8, pp. 2733–2744, 2001.

[14] W. Cui, L. Feng, C. Xu, S. Lü, and F. Qiu, "Hydrogen production by photocatalytic decomposition of methanol gas on Pt/TiO_2 nano-film," *Catalysis Communications*, vol. 5, no. 9, pp. 533–536, 2004.

[15] M. Zäch, C. Hägglund, D. Chakarov, and B. Kasemo, "Nanoscience and nanotechnology for advanced energy systems," *Current Opinion in Solid State and Materials Science*, vol. 10, no. 3–4, pp. 132–143, 2006.

[16] K. Hashimoto, T. Kawai, and T. Sakata, "Photocatalytic reactions of hydrocarbons and fossil fuels with water. Hydrogen production and oxidation," *Journal of Physical Chemistry*, vol. 88, no. 18, pp. 4083–4088, 1984.

[17] R. Dlugi and H. Gusten, "The catalytic and photocatalytic activity of coal fly ashes," *Atmospheric Environment*, vol. 17, no. 9, pp. 1765–1771, 1983.

[18] R. F. Lee, "Photo-oxidation and photo-toxicity of crude and refined oils," *Spill Science and Technology Bulletin*, vol. 8, no. 2, pp. 157–162, 2003.

[19] J. G. Fang and G. H. Xu, "Research progress in the synthesis of oxalate," *Chemical Propell & Poly Mater*, vol. 2, no. 2, pp. 18–21, 2004.

[20] M. M. Rauhut, L. G. Bollyky, and B. G. Roberts, "Chemilum inescence from reactions of electrtro-negatively substituted aryl oxalates with hydrogen peroxide and fluorescent compounds," *Journal of the American Chemical Society*, vol. 89, no. 25, pp. 6515–6522, 1967.

[21] D. M. Fenton and P. J. Steinwand, "Preparation of oxalates," 1967, US P 3393136.

[22] D. M. Fenton and P. J. Steinwand, "Noble metal catalysis IV preparation of dialkyl oxalates by oxidative carbonylation," *Journal of Organic Chemistry*, vol. 39, no. 5, pp. 701–703, 1974.

[23] H. S. Xie, Y. R. Zhu, A. M. Li, and L. Lu, "Application of TiO_2 powder in treating wastewater from paper-making factory," *Photographic Science and Photochemistry*, vol. 24, no. 4, pp. 312–317, 2006.

[24] S. W. Bi, B. Wang, and Y. Z. Gao, "Mechanistic study on reaction of $[Cp*Rh(CO)_2Me]BF_4$ with NBD," *Chinese Journal of Inorganic Chemistry*, vol. 22, no. 1, pp. 13–20, 2006.